Si(bzimpy)$_2$ – A Hexacoordinate Silicon Pincer Complex for Electron Transport and Electroluminescence

SCHOLARONE™
Manuscripts

Journal Name

COMMUNICATION

Si(bzimpy)₂ – A Hexacoordinate Silicon Pincer Complex for Electron Transport and Electroluminescence

Margaret Kocherga,[a] Jose Castaneda,[b] Michael G. Walter,[a] Yong Zhang,[b] Nemah-Allah Saleh,[a] Le Wang,[a] Daniel S. Jones,[a] Jon Merkert,[a] Bernadette Donovan-Merkert,[a] Yanzeng Li,[c] Tino Hofmann,[c] and Thomas A. Schmedake[a],*

A neutral hexacoordinate silicon complex containing two 2,6-bis(benzimidazol-2'-yl)pyridine (bzimpy) ligands has been synthesized and explored as a potential electron transport layer and electroluminescent layer in organic electronic devices. The air and water stable complex is fluorescent in solution with a λ_{max} = 510 nm and a QY = 57%. Thin films grown via thermal evaporation also fluoresce and posses an average electron mobility of 6.3×10^{-5} cm²/Vs. An ITO/Si(bzimpy)₂/Al device exhibits electroluminescence with λ_{max} = 560 nm.

Metal chelates such as tris(8-hydroxyquinolinato)aluminium, Alq₃, have been frequently used as electroluminescent layers (ELs) and/or as electron transport layers (ETLs) in a wide range of organic and hybrid electronic devices ever since the first efficient organic light emitting diode (OLED) device was reported by Tang and VanSlyke.[1] In addition to being a workhorse of the OLED field, Alq₃ and related metal chelates[2] are routinely used in organic solar cells,[3] perovskite solar cells,[4] memory /spintronic devices[5] and many other organic and hybrid electronic devices. In recent years, there has been a sustained interest in developing new materials for organic electronic devices, and there is particularly a need for new low molecular weight, chemically and electrochemically robust, ETL materials. The tetravalent silicon center provides the opportunity to explore a Si(ligand)₂ design, consisting of two dianionic pincer ligands. This design could provide greater stability, low molecular weights, low dipole moments, and the opportunity to tune redox and optical properties through synthetic design of the pincer ligand. Furthermore, the D₂d symmetry of the complex avoids the disadvantage of structural isomerism inherent in the M(ligand)₃ motif. The small

tetravalent silicon acts as a powerful Lewis acid significantly lowering the reduction potentials of the pincer ligands.[6] Also, the silicon center is fairly redox innocent with reductions being primarily ligand localized in hexacoordinate Si(IV) complexes.[7] These factors should lead to more efficient electron injection, greater intermolecular electronic coupling with low reorganization energies, and therefore fast electron transfer rates and high electron mobility.

We report the successful synthesis and characterization of a neutral, hexacoordinate silicon-based fluorescent complex **Si(bzimpy)₂** containing the palindromic, dianionic pincer ligand, 2,6-bis(benzimidazol-2'-yl)pyridine. Si(bzimpy)₂ was synthesized by adding SiCl₄ to a chloroform solution containing two equivalents of the bzimpy ligand and 4 equivalents of triethylamine, as HCl scavenger (Scheme 1). Upon injection of the SiCl₄, the blue luminescence of the free bzimpy ligand rapidly changes to an orange luminescence then finally a green luminescence for the 2:1 complex. Si(bzimpy)₂ precipitates out of the reaction, and subsequent Soxhlet extraction with chloroform provides a yellow powder in 38% yield. NMR provides clear evidence for the 2:1 hexacoordinate complex in solution. The D₂d symmetry results in a simple ¹H-NMR spectrum with only six ¹H signals. Notably, the aromatic H at the C7 position of the benzimidazole ring is considerably shielded (δ=5.75 ppm) by the aromatic ring current from the
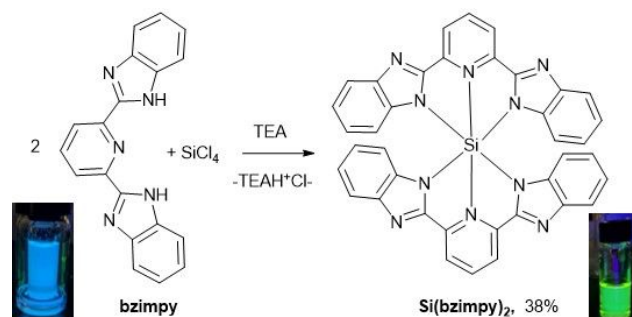
Scheme 1.

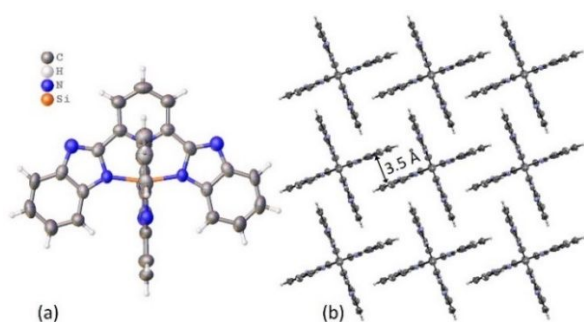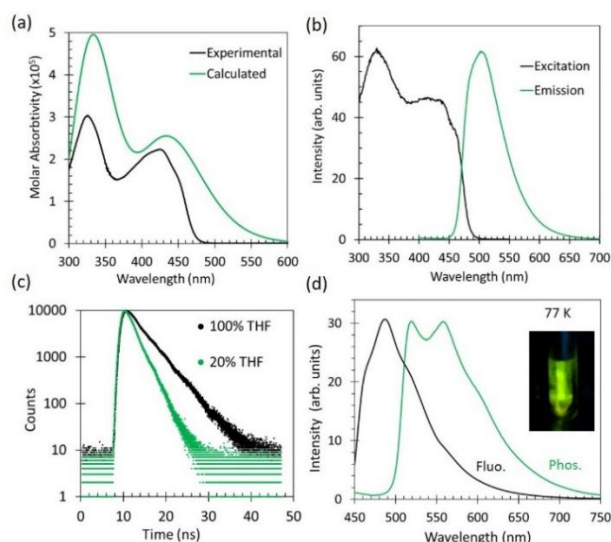**Figure 1.** (a) Crystal structure of Si(bzimpy)$_2$ in space group $P\overline{4}n2$, with solvent omitted for clarity. (b) Partial packing diagram of Si(bzimpy)$_2$ showing 2-dimensional layer.

Figure 2. (a) UV-vis experimental (black) and theoretical (green) spectrum for Si(bzimpy)$_2$ in CH$_2$Cl$_2$. (b) Fluorescence excitation (black) and emission (green) spectra in CH$_2$Cl$_2$ at RT. (c) Fluorescence lifetime of Si(bzimpy)$_2$ in THF (black) and THF/water - 20/80 (green). (d) Phosphorescence (green) and fluorescence (black) of Si(bzimpy)$_2$ in 2-methyl-THF at 77 K.

pyridine ring of the other perpendicular bzimpy ligand, as expected for the 2:1 hexacoordinate complex. Also, the ^{29}Si-NMR peak is consistent with a hexacoordinate silicon complex: ^{29}Si (CDCl$_3$-CD$_3$OD 40/60, 99MHz): δ -185.7 ppm.

Single crystals suitable for X-ray analysis were obtained via slow evaporation from a mixture of chloroform and methanol. The crystal structure (Figure 1) shows the bzimpy ligands adopt a planar, meridional arrangement, confiriming the positioning of the C7-H over the aromatic ring current of the pyridine group. Most noteworthy is the short Si-N$_{pyr}$ bond (1.874(5) Å) that is nearly the same length as the Si-N$_{imid}$ bond (1.870(5) Å). This is shorter than the range of Si-N bond lengths seen in previously reported hexacoordinate silicon complexes with unsubstituted pyridine ligands (1.93–2.02 Å), and it is even shorter than the Si-N bond length range (1.90-1.92 Å) seen with the very basic dimethylaminopyridine (DMAP) ligand.[8] This anomalously short Si-N$_{pyr}$ bond is likely a result of the geometric constraints placed by the meridional arrangement of the bzimpy ligand. With the short Si-N$_{pyr}$ bond and the small Si(IV) center, the Si(bzimpy)$_2$ complex is able to achieve a nearly octahedral geometry, ∠(N$_{imid}$-Si-N$_{imid}$) = 164.2(3)°. The packing diagram shows significant overlap of benzimidazole rings with interplanar distance of 3.5 Å. The close proximity of the aromatic rings could be beneficial for electron transport.

One of the advantages of pincer ligands is the thermal stability they impart on their metal complexes. The Si(bzimpy)$_2$ complex is very stable, likely due to the rigid tridentate nature of the bzimpy ligand. Thermogravimetric analysis confirmed the complex survived heating in nitrogen atmosphere to over 400 °C before thermal decomposition (ESI). Also, there was no evidence of hydrolysis of Si(bzimpy)$_2$ in mixed solvent solutions containing water. However, the reduced state of Si(bzimpy)$_2$ does not appear to be chemically stable. Cyclic voltammetry of Si(bzimpy)$_2$ in acetonitrile exhibited a chemically irreversible reduction wave with an onset around E$_{red, onset}$=-1.45 V and a peak current at E$_{red,pk}$ =-1.54 V vs. Fc$^+$/Fc at 200 mV/s (ESI). No oxidation wave was observed within the solvent window for acetonitrile. The chemical reactivity of the reduced species stands in contrast to some related hexacoordinate silicon complexes with polypyridine,[7a,b] porphyrin,[7c] and phenalene[7d,e]

ligands, which exhibit well-behaved, reversible, one-electron reduction waves.

A solution of Si(bzimpy)$_2$ in dichloromethane absorbs in the UV-vis with major bands at λ$_{max}$ = 325 nm and λ$_{max}$ = 427 nm. (Figure 2). The experimentally obtained UV-Vis spectrum correlates well with the calculated spectrum (TD-DFT, B3LYP/6-31g*, no solvent correction). Si(bzimpy)$_2$ emits in solution with a broad emission band centered at 510 nm. A degassed solution of Si(bzimpy)$_2$ in dry THF possessed a quantum yield, Φ = 57% and a lifetime, τ = 4.3 ns. Radiative and nonradiative rates were calculated for Si(bzimpy)$_2$ using the relationships shown in equation 1 (k$_{rad}$ = 1.3×10^8 s^{-1} and k$_{nr}$ = 1.0×10^8 s^{-1}). Addition of water led simultaneously to a decrease in the quantum yield and lifetime of the Si(bzimpy)$_2$, which indicates water decreases the radiative (k$_{rad}$) and increases the nonradiative (k$_{nr}$) relaxation rates (ESI, Table 3). The increase in k$_{nr}$ suggests that although the ground state is resistant to hydrolysis, the photoexcited state may be moisture sensitive.

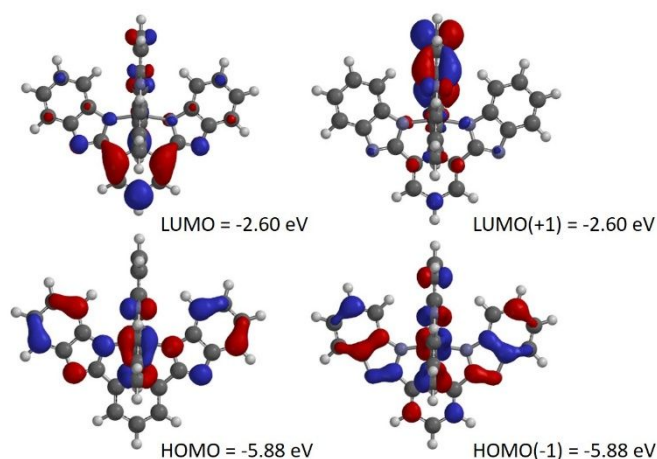$$\Phi = \frac{k_{rad}}{k_{rad} + k_{nr}} \quad \text{and} \quad \tau = \frac{1}{k_{rad} + k_{nr}} \quad \text{(equation 1)}$$

A solution of Si(bzimpy)$_2$ in 2-methyl-THF was frozen to 77 K to further probe the excited state properties. In the frozen glass, solvent relaxation is prevented, leading to a blue shift in the steady-state fluorescence spectrum and well-resolved transitions, with a λ$_{max}$ = 489 nm and unresolved shoulders around 463, 519, and 565 nm. Upon turning off the UV excitation, the frozen sample continues to visibly phosphoresce for several seconds. A spectrum of the phosphorescence shows two peaks at 520 and 561 nm and an
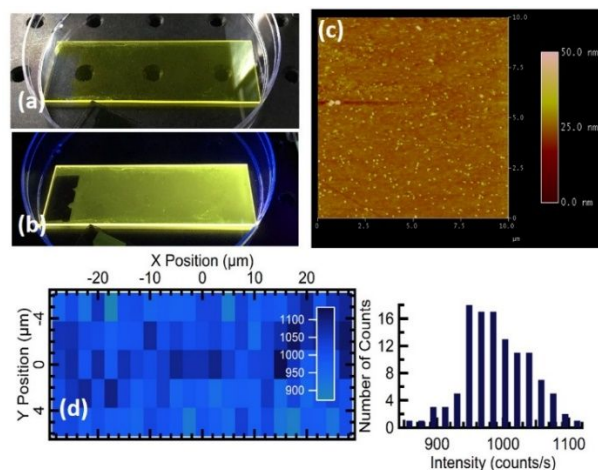
unresolved shoulder around 600 nm. The high triplet energy state, E_T= 2.38 eV, and low singlet-triplet energy gap, ΔE_{ST} = 294 meV are promising for triplet exciton device engineering (calculated using spectroscopic 0,0 transition values for $S_1 \rightarrow S_0$ and $T_1 \rightarrow S_0$ of 463 nm and 520 nm respectively).

Theoretical modelling of Si(bzimpy)$_2$ was performed using DFT with B3LYP/6-31G* functional and basis set and provided results consistent with the experimental observations. Geometry optimization provides a structure consistent with the obtained crystal structure, and calculated ^{1}H-NMR shifts predict the large upfield shift for the C7-^{1}H peak. TD-DFT calculations also adequately reproduce the observed UV-vis spectrum (figure 2a). Modelling predicts both the HOMO and LUMO are nearly double degenerate, with the HOMOs mostly localized on the benzimidazole rings and the LUMOs mostly localized on the pyridine ring (figure 3). The complex can be described as a simple push-pull system with silicon enhancing delocalization by enforcing planarity, which suggests further synthetic tuning of the optical properties of Si(pincer)$_2$ complexes will be possible through rational design. Furthermore, the theoretical gas phase E(LUMO) level at -2.6 eV compares reasonably well with the experimentally estimtated E(LUMO) = -3.4 eV determined from CV experiments, E(LUMO) =-e[$E_{red, onset}$ + 4.8V]).

As predicted, Si(bzimpy)$_2$ is easy to evaporate and deposit due to the low molecular weight and negligible dipole moment. Thin films were grown on silica glass substrates using a glovebox-integrated thermal deposition system. The deposited films are optically non-scattering and strongly colored (see figure 4a) and they are luminescent under UV excitation (figure 4b). Fluorescence spectroscopy of the film indicates a slight red-shift in the emission relative to solution to a λ_{max} = 549 nm (ESI). AFM analysis of a 64 nm thick film indicated a root mean square roughness R_{rms} = 2.8 nm and a mean roughness of 1.6 nm (figure 4c). Fluorescence imaging of the deposited film also indicated a smooth surface with uniform PL intensity ranging less than 10% (figure 4d).
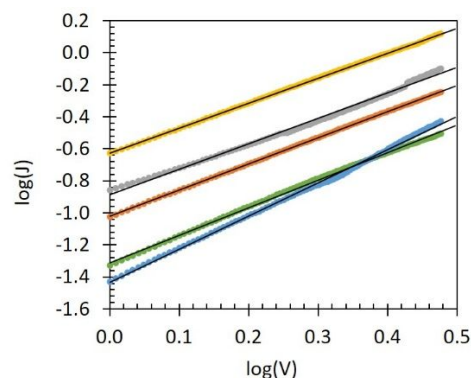

Figure 4. Thin film of Si(bzimpy)$_2$ deposited on glass slide under (a) ambient lighting and (b) UV illumination. (c) AFM of Si(bzimpy)$_2$ surface. (d) Fluorescence image and intensity histogram of Si(bzimpy)$_2$ film.

To explore the charge transport properties of the new compound, thin films of Si(bzimpy)$_2$ were grown on ITO followed by deposition of an aluminium contact. The thickness of the films were determined to be 64.1±0.2 nm with a substrate/film intermix of 5.7±0.5 nm according to spectroscopic ellipsometry over the range 0.65 to 4.1 eV. A log(J)-log(V) plot of the devices shows linear behaviour (R^2>0.99) over the 1-3 V region with slopes ranging between 1.6 and 2.1 consistent with a space charge limited current, SCLC regime (ESI). The charge mobility of Si(bzimpy)$_2$ was calculated from the slopes of the J vs. V^2 curves (Figure 5) of the devices in the SCLC region according to the Mott-Gurney equation (equation 2),[9] with L=64 nm and ε=3. The five samples gave an average μ = 6.3×10^{-5} cm^2/Vs with a standard deviation of 3.4×10^{-5} cm^2/Vs (ambient temperature and applied field of 1.5×10^5 – 7.8×10^5 V/cm). This value is comparable to the electron mobility of Alq$_3$ which was reported as 1.4×10^{-6} cm^2/Vs (ambient temperature and applied field of 4×10^5 V/cm).[10] The spread in mobility values

Figure 3. Calculated HOMO and HOMO-1 (left) and LUMO and LUMO+1 (right) of Si(bzimpy)$_2$ calculated in the gas phase, B3LYP/6-31G*, (Spartan 2016).

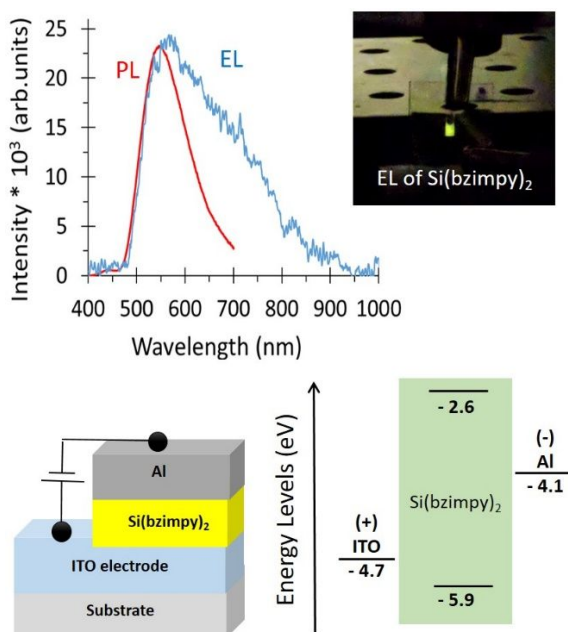**Figure 5.** Charge mobility curves for Si(bzimpy)$_2$ thin films (64 nm) sandwiched between ITO and Al. Calculated mobilities (cm^{2}V^{-1}s^{-1}) for each device were (gold) 1.2×10^{-4}, (gray) 7.1×10^{-5}, (orange) 5.2×10^{-5}, (blue) 4.3×10^{-5}, and (green) 2.9×10^{-5}.

COMMUNICATION

Figure 6. Spectrum of Si(bzimpy)$_2$ thin film PL (red) and EL (blue) of ITO/Si(bzimpy)$_2$/Al OLED device. Inset shows device in operation with yellow-green emission, from which EL spectrum was obtained. Bottom of figure shows the device design and energy diagram.

could result from variations in film quality, crystallinity and orientation and is the subject of further exploration.

$$J = \frac{9}{8}\varepsilon\varepsilon_o\mu\frac{V_a^2}{L^3} \qquad \text{equation 2}$$

A simple single-layer OLED consisting exclusively of Si(bzimpy)$_2$ sandwiched between ITO and Al was fabricated as shown in figure 6. Application of 12 V resulted in a yellow-green emission, with a λ_{max} = 560 nm. The unprotected devices lasted about 1 minute in a nitrogen filled glovebox before failing. This successful demonstration of a single-layer Si(bzimpy)$_2$ OLED device demonstrates the feasibility of Si(pincer)$_2$ complexes as candidates for charge transport and/or electroluminescent materials in organic electronic devices. Further device optimization is needed before attempting to ascertain the effect of Si(bzimpy)$_2$ on device performance. Nevertheless, this device confirms Si(pincer)$_2$ complexes are a promising new class of metal chelates for organic electronic devices, and the rich synthetic diversity of dianionic pincer ligands should provide a number of desirable and tailorable complexes for electron transport and electroluminescence applications.

Acknowledgements

Conflicts of interest

There are no conflicts of interests to declare.

Notes and references

1   C. W. Tang and S. A. VanSlyke, *Appl. Phys. Lett.*, 1987, **51**, 913-915.
2   (a) V. A. Montes, R. Pohl, J. Shinar and P. Anzenbacher, *Chem. Eur. J.,* 2006, **12**, 4523-4535. (b) V. M. Manninen, W. A. E. Omar, J. P. Heiskanen, H. J. Lemmetyinen and O. E. O. Hormi, *J. Mater. Chem.*, 2012, **22**, 22971-22982. (c) S. H. Liao, J. R. Shiu, S. W. Liu, S. J. Yeh, Y. H. Chen, C. T. Chen, T. J. Chow and C. I. Wu, *J. Am Chem. Soc.*, 2009, **131**, 763-777. (d) P. K. Nayak, N. Agarwal, F. Ali, M. P. Patankar, K. L. Narasimhan and N. Periasamy, *J. Chem. Sci.*, 2010, **122**, 847-855. (e) W. A. E. Omar, H. Haverinen and O. E. O. Hormi, *Tetrahedron*, 2009, **65**, 9707-9712. (f) C. Perez-Bolivar, S. Y. Takizawa, G. Nishimura, V. A. Montes and P. Anzenbacher, *Chem. Eur. J.,* 2011, **17**, 9076-9082.
3   (a) H. S. Kim, C. H. Kim, C. S. Ha and J. K. Lee, *Synth. Met.*, 2001, **117**, 289-291. (b) Q. L. Song, F. Y. Li, H. Yang, H. R. Wu, X. Z. Wang, W. Zhou, J. M. Zhao, X. M. Ding, C. H. Huang and X. Y. Hou, *Chem. Phys. Lett.*, 2005, **416**, 42-46. (c) F. F. Muhammad, M. Y. Yahya and K. Sulaiman, *Mater. Chem. Phys.*, 2017, **188**, 86-94.
4   (a) M. Mendez and E. Palomares, *RSC Adv.,* 2017, **7**, 35525-35527. (b) L. J. Chen, G. Wang, L. B. Niu, Y. Q. Yao, Y. X. Guan, Y. T. Cui and Q. L. Song, *RSC Adv.,* 2018, **8**, 15961-15966. (c) X. L. Ou, J. Feng, M. Xu and H. B. Sun, *Opt. Lett.*, 2017, **42**, 1958-1961.
5   (a) T. Abhijith, T. V. A. Kumar and V. S. Reddy, *Nanotechnology*, 2017, **28**, 095203. (b) C. Barraud, P. Seneor, R. Mattana, S. Fusil, K. Bouzehouane, C. Deranlot, P. Graziosi, L. Hueso, I. Bergenti, V. Dediu, F. Petroff and A. Fert, *Nat. Phys.*, 2010, **6**, 615-620. (c) V. Dediu, L. E. Hueso, I. Bergenti, A. Riminucci, F. Borgatti, P. Graziosi, C. Newby, F. Casoli, M. P. De Jong, C. Taliani and Y. Zhan, *Phys. Rev. B*, 2008, **78**, 115203. (d) K. Sugi, H. Ishii, Y. Kimura, M. Niwano, E. Ito, Y. Washizu, N. Hayashi, Y. Ouchi and K. Seki, *Thin Solid Films*, 2004, **464**, 412-415. (e) F. J. Wang, Z. H. Xiong, D. Wu, J. Shi and Z. V. Vardeny, *Synth. Met.*, 2005, **155**, 172-175. (f) C. H. Tu, Y. S. Lai and D. L. Kwong, *IEEE Electron Device Lett.*, 2006, **27**, 354-356. (g) J. G. Park, W. S. Nam, S. H. Seo, Y. G. Kim, Y. H. Oh, G. S. Lee and U. G. Paik, *Nano Letters*, 2009, **9**, 1713-1719.
6   B. Suthar, A. Aldongarov, I. S. Irgibaeva, M. Moazzen, B. T. Donovan-Merkert, J. W. Merkert and T. A. Schmedake, *Polyhedron,* 2012, **31**, 754-758.
7   (a) D. M. Peloquin, D. R. Dewitt, S. S. Patel, J. W. Merkert, B. T. Donovan-Merkert and T. A. Schmedake, *Dalton Trans.*, 2015, **44**, 18723-18726. (b) J. England and K. Wieghardt, *Inorg. Chem.*, 2013, **52**, 10067-10079. (c) C. R. Lorenz, H. D. Dewald and F. R. Lemke, *Electroanalysis*, 1997, **9**, 1273-1277. (d) S. K. Pal, M. E. Itkis, F. S. Tham, R. W. Reed, R. T. Oakley and R. C. Haddon, *J. of the Am. Chem. Soc.*, 2008, **130**, 3942-3951. (e) A. Sarkar, F. S. Tham and R. C. Haddon, *J. Mater. Chem.*, 2011, **21**, 1574-1581.
8   D. M. Peloquin and T. A. Schmedake, *Coord. Chem. Rev.*, 2016, **323**, 107-119.
9   V. Coropceanu, J. Cornil, D. A. da Silva, Y. Olivier, R. Silbey and J. L. Bredas, *Chemical Reviews*, 2007, **107**, 926-952.
10 R. G. Kepler, P. M. Beeson, S. J. Jacobs, R. A. Anderson, M. B. Sinclair, V. S. Valencia and P. A. Cahill, *Applied Physics Letters*, 1995, **66**, 3618-3620.